https://doi.org/10.48048/tis.2023.5649

Antibacterial Activities of Biosynthesized Zinc Oxide Nanoparticles and Silver-Zinc Oxide Nanocomposites using *Camellia Sinensis* Leaf Extract

Pankaj Kumar Jha[1,3,*], Chamorn Chawengkijwanich[2], Chonlada Pokum[2], Pichai Soison[2] and Kuaanan Techato[3]

[1]Department of Pharmaceutical Chemistry, Faculty of Pharmaceutical Sciences, Prince of Songkla University, Songkhla 90110, Thailand
[2]National Nanotechnology Center, National Science and Technology Development Agency, Thailand Science Park, Pathum Thani 12120, Thailand
[3]Faculty of Environmental Management, Prince of Songkla University, Songkhla 90110, Thailand

([*]Corresponding author's e-mail: nanoscience.jha.pankaj@gmail.com)

Received: 17 August 2022, Revised: 16 October 2022, Accepted: 23 October 2022, Published: 15 January 2023

Abstract

Green route of nanomaterials synthesis is increasing in demand due to ecofriendly to the environment. In this research, objective is to biosynthesize and evaluate the antibacterial performance of pure ZnO and Ag/ZnO nanocomposites using *Camellia sinensis* leaf extracts. Pure ZnO nanoparticles and Ag/ZnO nanocomposites were synthesized using *Camellia sinensis* leaf extract. The antibacterial effectiveness against gram-positive (*Staphylococcus aureus*) and gram-negative (*Escherichia coli*) bacteria were examined and compared with 1 % Chlorox as a commercial disinfectant by well diffusion method based on the zone of inhibition. Pure ZnO nanoparticles and Ag/ZnO nanocomposites had hexagonal shape ZnO nanoparticles and rectangular shape Ag nanoparticles in Ag/ZnO nanocomposites with a particle crystal size between 20 - 30 nm with carboxylic and phenolic functional group attached on it. Ag/ZnO nanocomposites exhibited antibacterial effectiveness against both gram-positive and gram-negative bacteria, while pure ZnO nanoparticles exhibited antibacterial effectiveness against only gram-positive bacteria. Conversely, 1 % Chlorox and 1 % DMSO showed no significant antibacterial activity against gram-positive and gram-negative bacteria. *Camellia sinensis* mediated ZnO and Ag/ZnO nanoparticles showed antibacterial potential against *S. aureus* and *E. coli* suggesting that green route to synthesis of antibacterial nanoparticles can be an excellent strategy to develop eco-friendly disinfectant products.

Keywords: Biosynthesis, ZnO nanocomposites, Antibacterial resistant, Gram negative bacteria, Gram positive bacteria, Disinfectant, Household materials

Introduction

Today's global healthcare challenge is antimicrobial resistance [1]. In cleaning and disinfecting household materials, commercial disinfectants like citric acid ($C_6H_{10}O_8$), quaternary ammonium compounds, potassium peroxymonosulfate ($KHSO_5$), sodium dichloroisocyanurate ($C_3Cl_2N_3NaO_3$) and glutaraldehyde ($C_5H_8O_2$) are less effective in microbially contaminated surfaces [2]. Most hospitals are a major source of microbial pollutants due to large numbers of various microbial disease infected patients [3]. It has been shown that equipment and diagnostic instruments in hospitals have a high risk of microbial contaminants [4].

Nanotechnology is an emerging field of study which explores the nanoscale level and its various applications [5]. Nanomaterials have size-dependent properties, i.e. lesser size has a higher toxic effect on bacteria, virus, cell membranes and vice versa [6]. It has been shown that size variations exhibit a variation of toxicity over gram-positive and gram-negative bacteria [7]. Among antimicrobial nanomaterials, zinc oxide (ZnO) and silver (Ag) nanoparticles have attracted an increasing amount of attention because of their various desirable properties such as optical properties, and size tunable properties. ZnO nanoparticles have biological activity, chemical stability, low cost and large surface area. ZnO nanoparticles exhibit antibacterial properties by redox oxygen species (ROS) formation in the cell wall of bacteria [8] and have been shown to exhibit efficient antibacterial effects on oral cavity microorganisms [9] and Ag/ZnO nanocomposites have shown an even higher antibacterial effect [10]. In dark conditions, Ag^+ ions and Zn^{2+}

ions attack on the bacterial cell membrane and rupture the cell; however, the actual mechanism is unknown [11,12].

Several chemical or physical methods of nanoparticles synthesis have been reviewed [13]. These methods often require chemical substances and expensive or complex procedures such as laser ablation, physical vapor deposition and chemical vapor deposition. In recent years, biosynthesis i.e., green synthesis of metal nanoparticles has become an interesting alternative method due to phytochemicals present in the biological substances being able to act as a reducing and capping agent, enhancing life span of nanoparticles that overcome limitations of chemical and physical methods [14]. Several studies have shown the synthesis of metal nanoparticles using plant, fungi and bacteria [15,16]. However, nanoparticles synthesis using plant extracts might be advantageous over other biological processes because it eliminates the elaborate process of maintaining cell cultures, leading to its suitability to be scaled up for large-scale nanoparticles synthesis. It is also eco-compatible and cost effective containing functional groups such as carboxylic acid, phenols, ketones, alcohols, alkenes, alkanes etc., which are reducing agent and capping agent in the process of nanoparticles formation.

Among various plants, *Camellia sinensis* (tea plant) is today cultivated across the world in tropical and subtropical regions even though it is native to East Asia, the Indian subcontinent and Southeast Asia. It has been shown that *Camellia sinensis* leaf content consists of alcohol, phenols, amines, carboxylic acid, polyphenols, polysaccharides and amino acid which acts as reducing and stabilizing agents in ZnO nanomaterials formation [17]. Variation of pH during the hydrothermal synthesis has also resulted in the formation of different ZnO nanomaterial structures [18]. Rod structures occur below pH 8 whereas nanotetrapod structures like flowers and sea urchins occur between pH 8 to 12. Furthermore, biosynthesis method at different pH is still of interest for controlled toxicity studies over clinical pathogenic bacteria to minimize antibacterial resistant problem [19].

The objective of the present work was to biosynthesize pure ZnO nanoparticles and Ag/ZnO nanocomposites at pH 5 using *C. sinensis* leaf extract and to evaluate their antibacterial activities on gram-negative and gram-positive bacteria for hospital equipment disinfection purposes.

Materials and methods

Chemicals

Zinc nitrate hexahydrate ($Zn(NO_3)_2 \cdot 6H_2O$, purity ≥ 98 %) and silver nitrate ($AgNO_3$ purity ≥ 99.0 %) were purchased from Sigma-Aldrich and used as zinc precursor and silver precursor, respectively. Sodium hypochlorite (NaOCl, 10 %), dimethyl Sulfoxide (DMSO) and sodium hydroxide (NaOH) were purchased from Gammaco, Thailand. Nutrient agar (NA), muller hilton agar and peptone were purchased from Difco laboratories, USA.

Preparation of chemicals

A 1 % NaOCl solution was prepared by mixing 10 mL of 10 % NaOCl with 90 mL of deionized (DI) water to make 100 mL of solution. A 1 % DMSO solution was prepared by mixing 1 mL of DMSO with 99 mL of DI water. One millimolar (1 mM) of $AgNO_3$ solution was prepared by adding 0.0169 mg of $AgNO_3$ in 100 mL of DI water. One normality (1 N) of NaOH was prepared by mixing 4 g of NaOH pallets in 100 mL of DI water.

Preparation of leaf extract

Camellia sinensis normal dried leaves were purchased from a supermarket in Pathum Thani, Thailand. Dried leaves were washed with DI water prior to use for extraction according to the previous method [20] with some modifications such as air dry at room temperature after washing with DI water. Twenty-five g of dried leaves were mixed with 100 mL of DI water using magnetic stirrer for 20 min at 65 ℃. The leaf extract was then filtered with Whatman no. 1 filter paper and cooled at room temperature.

Biosynthesis of ZnO nanoparticles and Ag/ZnO nanocomposites

ZnO nanoparticles were synthesized by mixing 3 g of $Zn(NO_3)_2 \cdot 6H_2O$ with 40 mL of *Camellia sinensis* leaf extract (**Figure 1**). The mixture was added drop by drop with 1 N NaOH to reach pH 5 and boiling at 80 ℃ with continuous stirring [21] until the color changed from a reddish green to beige color and a paste formation appeared. The paste was dried on a hot plate at 80 ℃, crushed and annealed at 300 ℃ for 3 h.

Ag/ZnO nanocomposite was synthesized by adding 100 mL of 1 mM $AgNO_3$ solution and 3 g of $Zn(NO_3)_2 \cdot 6H_2O$ in 40 mL of *C. sinensis* leaf extract (**Figure 1**). The mixture was added drop by drop with

1 N NaOH to reach pH 5 and boiling at 80 ℃ with continuous stirring until the color changed from a reddish green to dark greenish brown color and a paste formation appeared. The paste was dried on a hot plate at 80 ℃, crushed and annealed at 300 ℃ for 3 h.

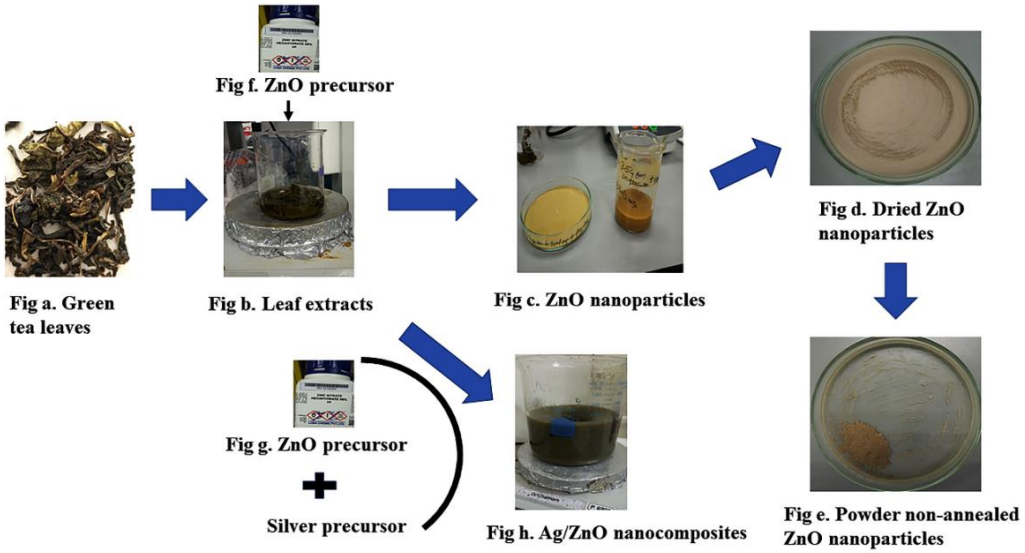

Figure 1 Schematic diagram of biosynthesis of ZnO nanoparticles and Ag/ZnO nanocomposites.

Antibacterial activities

Escherichia coli ATCC 8739 and *Staphylococcus aureus* ATCC 6538P strains were purchased from Thai Can Biotec Co., Ltd., Bangkok, Thailand. Nutrient agar (NA) media was prepared by mixing 2.3 g of NA powder with 100 mL of DI water. Muller Hilton agar (MHA) was prepared by mixing 15.2 g of MHA powder with 400 mL of DI water. Peptone water was prepared by mixing 1 g of peptone powder with 100 mL DI water and 1 N NaOH was added drop by drop to adjust its pH to 8.6 - 9.0 (alkaline condition). These prepared solutions were autoclaved at 121 ℃ for 15 min.

The antibacterial effectiveness against gram-positive *S. aureus* and gram-negative *E. coli* were examined and compared with 1 % Chlorox (NaOCl) as a commercial disinfectant by paper disc diffusion method. *Escherichia coli* and *Staphylococcus aureus* were cultured on different nutrient agar (NA) media plates at 37 ℃ for 24 h. One colony of *E. coli* ATCC 8739 and *S. aureus* ATCC 6538P bacteria were harvested and transferred into peptone water test tubes. Peptone water test tubes containing each bacterium were incubated for 20 min at room temperature. Twenty mL of MHA media were poured into a petri dish and solidified at room temperature. *E. coli* 8739 and *S. aureus* 6538P bacteria were then spread over MHA plates using a sterile swab. A whatman no.1 filter paper (5 mm in diameter) was placed on MHA agar and marked to load ZnO nanoparticles, Ag/ZnO nanocomposites, 1 % NaOCl and 1 % DMSO. Three mg of ZnO nanoparticles were added into 3 mL of 1 % DMSO solution to prepare 0.1 % ZnO concentration while 3 mg Ag/ZnO nanocomposites were added into 3 mL of 1 % DMSO solution to prepare 0.1 % Ag/ZnO concentration. Next, 40 µL of 0.1 % ZnO, 0.1 % Ag/ZnO and 1 % NaOCl were loaded onto the marked paper dish while 40 µL of 1 % DMSO was loaded as a control. The petri dishes were further incubated at 37 ℃ for 24 h. A zone of inhibition was measured for each antimicrobial agent similar to Nguyen *et al.* [22].

Characterizations

An ultraviolet-visible (UV-vis) Spectrophotometer (Perkin Elmer, model Lambda 650) was used to analyze the optical property of ZnO and Ag/ZNO based on absorption spectra with the wavelength range of 200 - 800 nm. ZnO and Ag/ZnO powder were separately mixed with DI water and sonicated for 5 min and then taken for UV-vis absorbance. Band gap energy was calculated using the formula similar to Shashanka *et al.* [23]:

$$Eg = \frac{hc}{\lambda} \quad (1)$$

where *'Eg'* is bandgap energy, *h* is Planck's constant 6.626×10^{-36} J·s, *'c'* is speed of light 3.8×10^{8} m/s and 'λ' is absorbance wavelength.

An X-Ray Diffractometer (XRD; Bruker, D8 Advance) was used for phase and purity analysis. The average crystal size was calculated using Scherer's equation similar to Sánchez-López *et al.* [24]:

$$D = \left[\frac{K\lambda}{\beta Cos\theta}\right] A° \quad (2)$$

where D is the average crystallite diameter in Angstrom, K is the Scherrer constant, λ is the wavelength of X-ray i.e. 1.5406 Å, CuKα radiation, Θ is the Braggs' angle and β is the full width at half maximum intensity of diffraction peak.

Fourier Transform Infrared Spectrophotometer (FTIR, IRTracer-100AH, Shimadzu) was used to measure the functional group attached on the surface of nanoparticles by recording spectrum from 400 to 4,000 cm^{-1} using ATR technique. Surface morphology and size of ZnO and Ag/ZnO samples were characterized by scanning microscopy (Model SU8030, HITACHI, Japan). Structure of the ZnO sample was characterized by transmission electron microscope (LEOL model JEM 2100).

Results and discussion

UV-visible analysis

The absorbance peak of Ag/ZnO nanocomposite showed at 378 nm confirming a decreasing frequency, which is a red shift. Red shift is the phenomena where frequency of the light seems to be decreasing or wavelength of the light seems to be increasing. Similarly, the absorbance peak of ZnO nanoparticles showed at 376 nm confirming increasing frequency, which is a blue shift (**Figure 2**). Blue shift is the phenomena where frequency of the light seems to be increasing or wavelength of the light seems to be decreasing. The band gap of Ag/ZnO nanocomposites showed 3.29 eV (**Figure 2**) and a band gap of ZnO nanoparticles showed 3.28 eV. Silver (Ag) nanoparticle increased band gap absorption performance ranges from conduction band and valence band by accelerating the light absorption capacity in Ag/ZnO nanocomposites, which is similar to the study by Zare *et al.* [25].

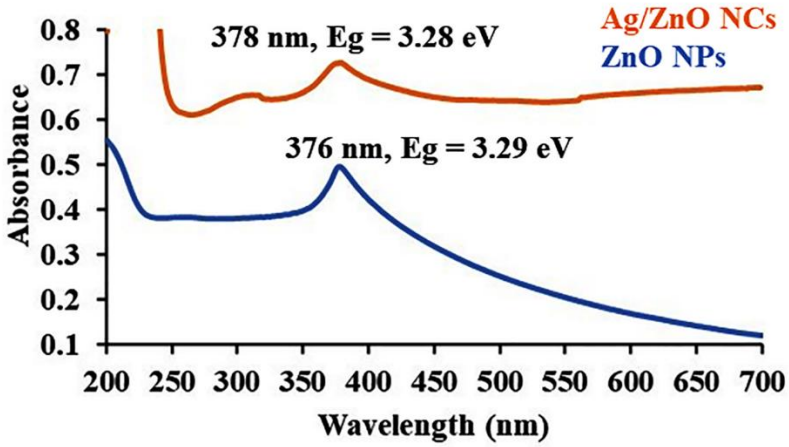

Figure 2 UV-vis absorbance analysis of ZnO nanoparticles and Ag/ZnO nanocomposites.

X-ray diffraction (XRD) analysis

Figure 3 shows XRD patterns of the biosynthesized ZnO nanoparticles and Ag/ZnO nanocomposite. Peaks corresponding to lattice plane (h, k and l) values of (100), (002) and (101) at the diffraction angle (2Θ) value 31.60, 34.45 and 36.21 ° for ZnO NPs whereas a lattice plane (h, k and l) value of (111) at the diffraction angle (2Θ) value 38 ° for Ag NPs. In Ag/ZnO nanocomposite XRD showed lattice spacing for Ag nanoparticle was 0.236 nm and crystal size 25.7 nm. Lattice spacing for ZnO nanoparticle was 0.282 nm and crystal size 28.8 nm. Overall Ag/ZnO nanocomposite has 71.2 % crystallinity and 28.8 % amorphousness.

In pure ZnO nanoparticles, XRD analysis showed lattice spacing of 0.282 nm and crystal size of 23.7 nm. Similarly, 79.7 % of crystallinity and 20.3 % amorphous, which is similar to the study by Taha *et al.* [26].

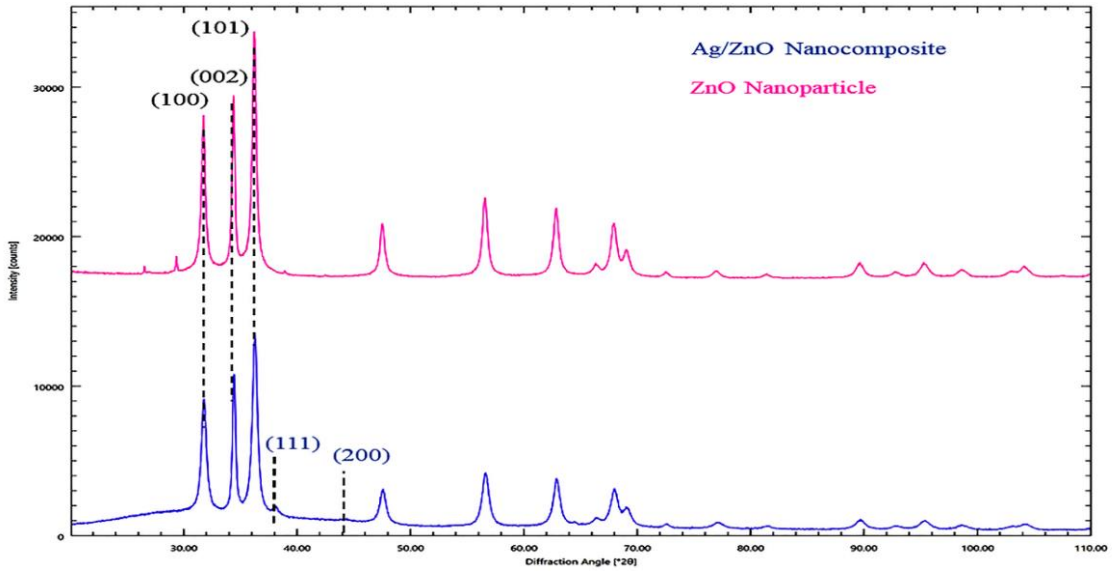

Figure 3 X-Ray Diffraction analysis of ZnO nanoparticles and Ag/ZnO nanocomposites.

Fourier Transform Infrared (FTIR) analysis

FTIR analysis showed a peak at 1,440, 1,371 and 881 wavenumbers (cm^{-1}) for ZnO nanoparticles and Ag/ZnO nanocomposites (**Figure 4**). Broad peak at 1,440 cm^{-1} showed O-H bending having Carboxylic acid. Medium O-H bending at 1,371 cm^{-1} showed Phenol and band at 881 cm^{-1} showed strong C-H bending, which is similar to the study by Balogun *et al.* [27].

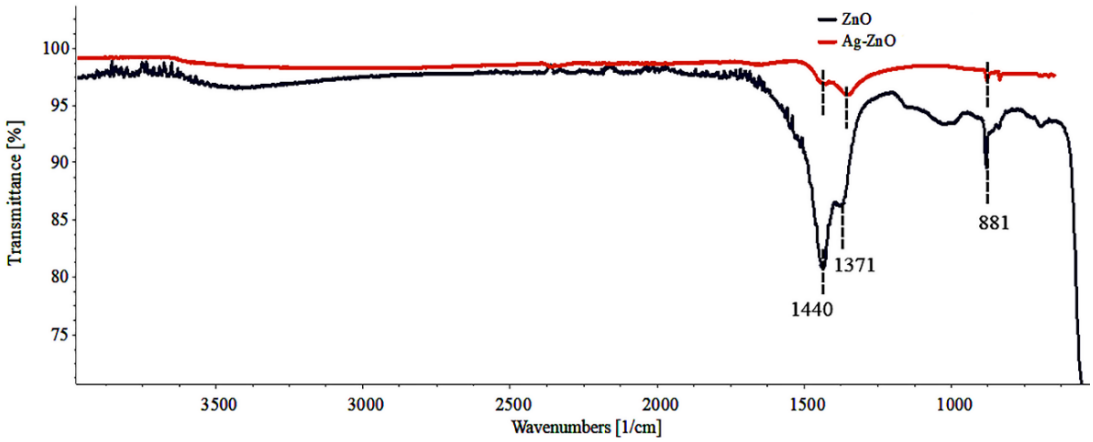

Figure 4 Furrier Transform Infrared (FTIR) analysis of ZnO nanoparticles and Ag/ZnO nanocomposites.

Scanning Electron Microscope (SEM) analysis

SEM analysis for ZnO nanoparticles and Ag/ZnO nanocomposites observed at magnification 100 k scale showed a hexagonal shape for ZnO nanoparticles in both samples and a rectangular shape for Ag nanoparticles in Ag/ZnO nanocomposites (**Figure 5**). In Ag/ZnO nanocomposites, the average size of Ag nanoparticles measured 86 nm and the average size for ZnO nanoparticles measured 90 nm. In pure ZnO nanoparticles, the average size for ZnO nanoparticles measured 89 nm, which is similar to Fageria *et al.* [28].

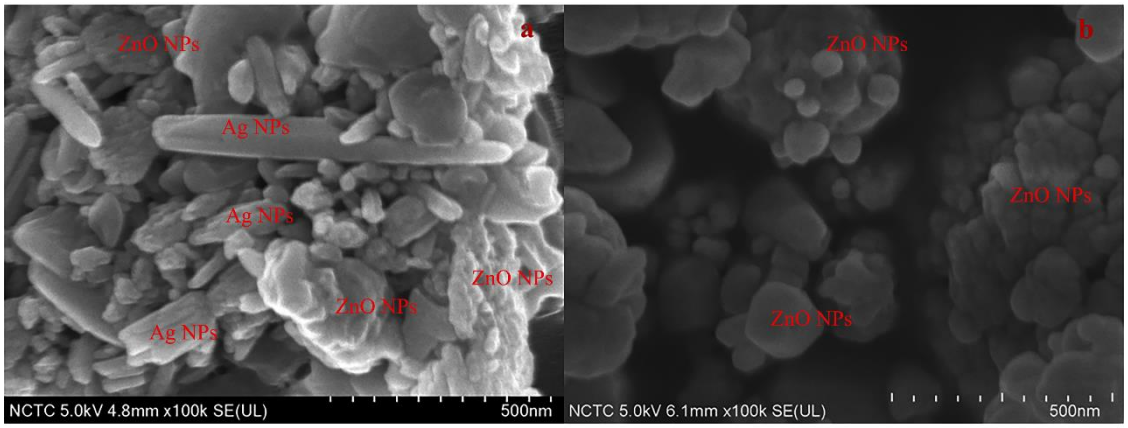

Figure 5 Scanning Electron Microscope (SEM) analysis (a) Ag/ZnO nanocomposites having 86 nm average width of Ag nanoparticles and 90 nm average diameter of ZnO nanoparticles, (b) Pure ZnO nanomaterials having 89 nm average diameter.

Transmission Electron Microscope (TEM) analysis

TEM analysis for ZnO nanoparticles confirmed the hexagonal structure (**Figure 6**). The average TEM image size at 200 nm scale measured 333 nm, a result similar to the study by Oo *et al.* [29].

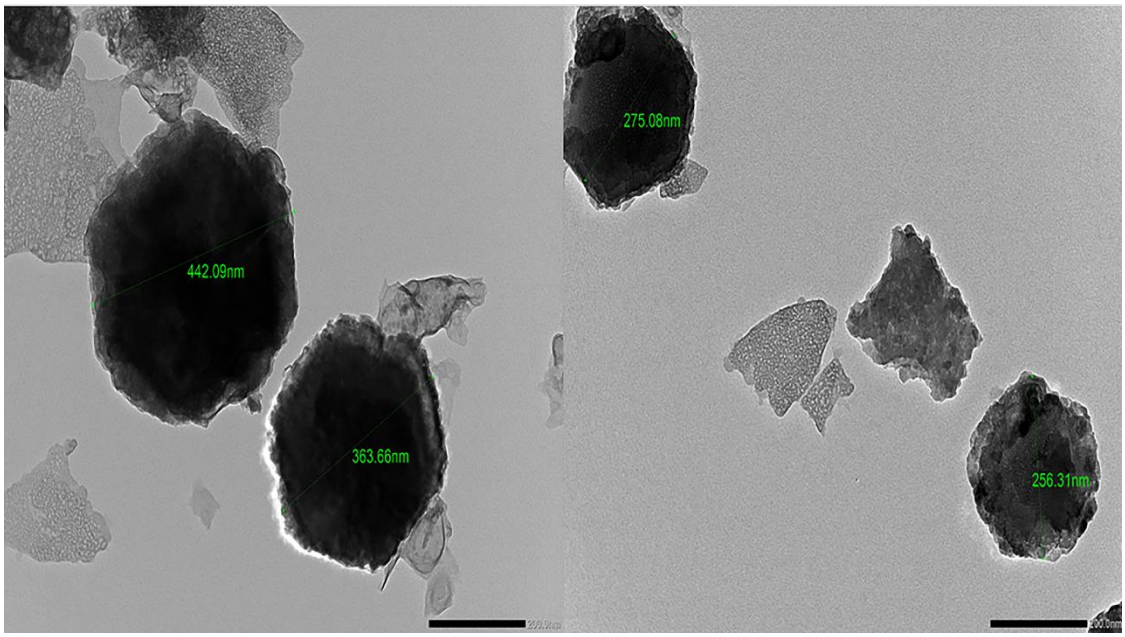

Figure 6 Transmission Electron Microscope (TEM) showing hexagonal shape for ZnO nanoparticles.

Antibacterial activities

The antibacterial property of biosynthesized ZnO and Ag/ZnO samples was tested using agar disc diffusion technique (**Figure 7**). Results demonstrated that ZnO and Ag/ZnO at 0.1 % concentrations exhibited an antibacterial effect against *S. Aureus*, but 1 % NaOCl and 1 % DMSO did not. NaOCl and DMSO showed no zone of inhibition in both *S. aureus* and *E. coli*. **Table 1** shows that Ag/ZnO nanocomposite exhibited a stronger antibacterial property than pure ZnO nanoparticles. Inhibition zones of Ag/ZnO samples were 13 ± 0.75 and 14 ± 0.74 mm against *E. coli* and *S. Aureus*, respectively. However, ZnO particles did not exhibit any antibacterial property against *E. Coli* at 0.1 % of ZnO nanoparticle concentration confirming resistant behaviour.

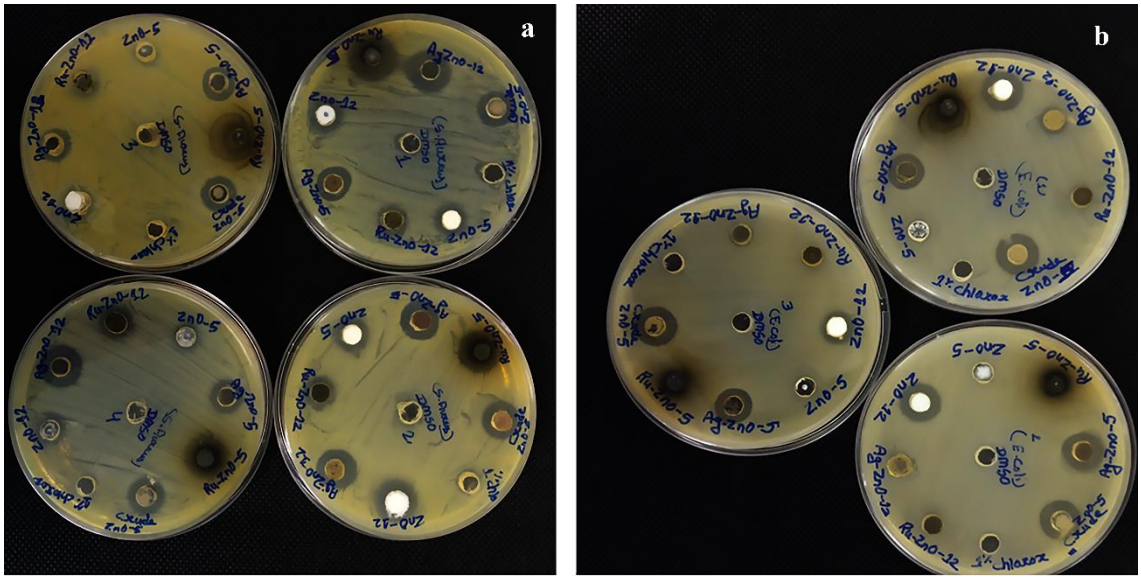

Figure 7 Zone of inhibition in a) *Staphylococcus aureus* ATCC 6538P, b) *Escherichia coli* ATCC 8739.

Table 1 Zone of inhibition shown in *S. aureus* and *E. coli* bacteria.

	0.1 % ZnO NPs		0.1 % Ag/ZnO NPs		1 % NaOCl	1 % DMSO
	Average	**SD**	**Average**	**SD**	**Average**	**Average**
E. coli ATCC 8739	0 mm		13 mm	± 0.75 mm	0 mm	0 mm
S. aureus ATCC 6538P	12 mm	± 1.75 mm	14 mm	± 0.74 mm	0 mm	0 mm

Conclusions

Green tea mediated biosynthesis of ZnO nanoparticles and Ag/ZnO nanocomposite at pH 5 and 80 ℃ temperature was synthesized. Scanning electron microscope analysis confirmed an average of 89 nm size in pure ZnO nanoparticles. Similarly, 86 nm size for Ag nanoparticles and 90 nm size for ZnO nanoparticles in Ag/ZnO nanocomposites was confirmed. XRD has confirmed the crystallinity. The antibacterial study showed that Ag/ZnO nanocomposites have higher antibacterial activity in comparison with ZnO nanoparticles on *S. aureus* ATCC 6538P bacteria. In *E. coli* ATCC 8739 bacteria, ZnO nanoparticles have no antibacterial effect, and it is due to low concentration 0.1 % of zinc nanoparticles where *E. coli* ATCC 8739 bacteria is resistant. Commercial disinfectant 1 % Chlorox (NaOCl) showed no antibacterial activity on both gram-positive and gram-negative bacteria due to resistant. In contrast, disinfection problem could be minimized using lower concentration of zinc oxide nanocomposites comparatively with sodium hypochlorite which is used in household microbial disinfection. In comparison between ZnO nanoparticle and Ag/ZnO nanocomposite, Ag/ZnO nanocomposite has better antibacterial effectiveness due to its lower band gap energy which helps to excite more numbers of electron with low energy and helps to form ROS binding in bacterial cell membrane. In conclusion, nanoparticles could be synthesized at pH 5 and 80 ℃ temperature for antimicrobial application.

Acknowledgements

We would like to thank the National Nanotechnology Center (NANOTEC), National Science Technology and Development Agency (NSTDA), Thailand Science Park, Thailand for financial support under grant N. P1751698. The authors are also grateful to Thailand Graduate Institute of Science and Technology (TGIST), National Science Technology and Development Agency (NSTDA), Thailand Science Park, Thailand for their support with contract no. SCA-CO-2562-9699-EN.

References

[1] CL Ventola. The antibiotic resistance crisis. Part 1: Causes and threats. *Pharm. Therapeut*. 2015; **40**, 277-83.

[2] Y Jang, K Lee, S Yun, M Lee, J Song, B Chang and NH Choe. Efficacy evaluation of commercial disinfectants by using *Salmonella enterica* serovar Typhimurium as a test organism. *J. Vet. Sci.* 2017; **18**, 209-16.

[3] J Wang, J Shen, D Ye, X Yan, Y Zhang, W Yang, X Li, J Wang, L Zhang and L Pan. Disinfection technology of hospital wastes and wastewater: Suggestions for disinfection strategy during coronavirus disease 2019 (COVID-19) pandemic in China. *Environ. Pollut.* 2020; **262**, 114665.

[4] JL Sagripanti and A Bonifacino. Bacterial spores survive treatment with commercial sterilants and disinfectants. *Appl. Environ. Microbiol.* 1999; **65**, 4255-60.

[5] H Bahadar, F Maqbool, K Niaz and M Abdollahi. Toxicity of nanoparticles and an overview of current experimental models. *Iran. Biomed. J.* 2016; **20**, 1-11.

[6] C Liao, Y Li and SC Tjong. Bactericidal and cytotoxic properties of silver nanoparticles. *Int. J. Mol. Sci.* 2019; **20**, 449.

[7] S Agnihotri, S Mukherji and S Mukherji. Size-controlled silver nanoparticles synthesized over the range 5-100 nm using the same protocol and their antibacterial efficacy. *RSC Adv.* 2014; **4**, 3974-83.

[8] A Sirelkhatim, S Mahmud, A Seeni, NHM Kaus, LC Ann, SKM Bakhori, H Hasan and D Mohamad. Review on zinc oxide nanoparticles: Antibacterial activity and toxicity mechanism. *Nano-Micro Lett.* 2015; **7**, 219-42.

[9] S Kasraei, L Sami, S Hendi, MY Alikhani, L Rezaei-Soufi and Z Khamverdi. Antibacterial properties of composite resins incorporating silver and zinc oxide nanoparticles on *Streptococcus mutans* and *Lactobacillus*. *Restor. Dent. Endod.* 2014; **39**, 109-14.

[10] J Shang, Y Sun, T Zhang, Z Liu and H Zhang. Enhanced antibacterial activity of Ag nanoparticle-decorated ZnO nanorod arrays. *J. Nanomater*. 2019; **2019**, 3281802.

[11] S Jiang, K Lin and M Cai. ZnO nanomaterials: Current advancements in antibacterial mechanisms and applications. *Front. Chem.* 2020; **8**, 580.

[12] Y Qing, L Cheng, R Li, G Liu, Y Zhang, X Tang, J Wang, H Liu and Y Qin. Potential antibacterial mechanism of silver nanoparticles and the optimization of orthopedic implants by advanced modification technologies. *Int. J. Nanomed.* 2018; **13**, 3311-27.

[13] I Ijaz, E Gilani, AF Nazir and A Bukhari. Detail review on chemical, physical and green synthesis, classification, characterizations and applications of nanoparticles. *Green Chem. Lett. Rev.* 2020; **13**, 223-45.

[14] M Naseer, U Aslam, B Khalid and B Chen. Green route to synthesize zinc oxide nanoparticles using leaf extracts of *Cassia fistula* and *Melia azadarach* and their antibacterial potential. *Sci. Rep.* 2020; **10**, 9055.

[15] JY Song, HK Jang and BS Kim. Biological synthesis of gold nanoparticles using *Magnolia kobus* and *Diopyros kaki* leaf extracts. *Process Biochem.* 2009; **44**, 1133-8.

[16] J Huang, Q Li, D Sun, Y Lu, Y Su, X Yang, H Wang, Y Wang, W Shao, N He, J Hong and C Chen. Biosynthesis of silver and gold nanoparticles by novel sundried *Cinnamomum camphora* leaf. *Nanotechnology* 2007; **18**, 105104.

[17] CD Medina, E Mostafavi, A Vernet-Crua, H Barabadi, V Shah, JL Cholula-Díaz, G Guisbiers and TJ Webster. Green nanotechnology-based zinc oxide (ZnO) nanomaterials for biomedical applications: A review. *J. Phys. Mater.* 2020; **3**, 034005.

[18] G Amin, MH Asif, A Zainelabdin, S Zaman, O Nur and M Willander. Influence of pH, precursor concentration, growth time, and temperature on the morphology of ZnO nanostructures grown by the hydrothermal method. *J. Nanomater.* 2011; **2011**, 5.

[19] K Chitra and G Annadurai. Antibacterial activity of pH-dependent biosynthesized silver nanoparticles against clinical pathogen. *Biomed. Res. Int.* 2014; **2014**, 725165.

[20] J Santhoshkumar, SV Kumar and S Rajeshkumar. Synthesis of zinc oxide nanoparticles using plant leaf extract against urinary tract infection pathogen. *Resour. Effic. Tech.* 2017; **3**, 459-65.

[21] S Alamdari, MS Ghamsari, C Lee, W Han, HH Park, MJ Tafreshi, H Afarideh and MHM Ara. Preparation and characterization of zinc oxide nanoparticles using leaf extract of *Sambucus ebulus*. *Appl. Sci.* 2020; **10**, 3620.

[22] NYT Nguyen, N Grelling, CL Wetteland, R Rosario and H Liu. Antimicrobial activities and mechanisms of magnesium oxide nanoparticles (nMgO) against pathogenic bacteria, yeasts, and biofilms. *Sci. Rep.* 2018; **8**, 16260.

[23] R Shashanka, H Esgin, VM Yilmaz and Y Caglar. Fabrication and characterization of green synthesized ZnO nanoparticle based dye-sensitized solar cells. *J. Sci. Adv. Mater. Device*. 2020; **5**, 185-91.

[24] P Sánchez-López, J Antúnez-García, S Fuentes-Moyado, DH Galván, V Petranovskii and F Chávez-Rivas. Analysis of theoretical and experimental X-ray diffraction patterns for distinct mordenite frameworks. *J. Mater. Sci.* 2019; **54**, 7745-57.

[25] M Zare, K Namratha, S Alghamdi, YHE Mohammad, A Hezam, M Zare, QA Drmosh, K Byrappa, BN Chandrashekar, S Ramakrishna and X Zhang. Novel green biomimetic approach for synthesis of ZnO-Ag nanocomposite; antimicrobial activity against food-borne pathogen, biocompatibility and solar photocatalysis. *Sci. Rep*. 2019; **9**, 8303.

[26] A Taha, MB Aissa and E Da'na. Green synthesis of an activated carbon-supported Ag and ZnO nanocomposite for photocatalytic degradation and its antibacterial activities. *Molecules* 2020; **25**, 1586.

[27] SW Balogun, OO James, YK Sanusi and OH Olayinka. G reen synthesis and characterization of zinc oxide nanoparticles using bashful (*Mimosa pudica*), leaf extract: A precursor for organic electronics applications. *SN Appl. Sci.* 2020; **2**, 504.

[28] P Fageria, S Gangopadhyay and S Pande. Synthesis of ZnO/Au and ZnO/Ag nanoparticles and their photocatalytic application using UV and visible light. *RSC Adv.* 2014; **4**, 24962-72.

[29] WMH Oo, MD McCluskey, AD Lalonde and M Norton. Infrared spectroscopy of ZnO nanoparticles containing CO_2 impurities. *Appl. Phys. Lett.* 2005; **86**, 073111.